Ab initio potential energy surfaces of HCS+: A study of the ground and the low-lying excited electronic states

Rajwant Kaur, T.J. Dhilip Kumar *

Department of Chemistry, Indian Institute of Technology Ropar, Rupnagar 140001, India

ABSTRACT

Three dimensional *ab initio* potential energy surfaces (PESs) have been computed for the ground state and low-lying excited states of HCS+ molecular ion using the internally contracted multi-reference (single and double) configuration interaction and augmented correlation consistent polarized valence quadruple zeta (aug-cc-pVQZ) basis sets. Ground state global PES is analyzed as dissociation of molecular ion into $H + CS^+$. The ground state PES ($H + CS^+$) has been fitted by the inverse power series expansion function. The anisotropy of the surface has been analyzed in terms of the multipolar expansion coefficients for the rigid-rotor surface. The surface will be useful for detailed understanding of collision dynamics in terms of ro-vibrational cross sections and rate coefficients.

1. Introduction

Chemical processes in the interstellar medium occurring due to the ion-neutral collisions play a fundamental role in the areas of molecular physics and astrophysics. Proton collision with diatomic molecules is important in atmospheric chemistry and combustion processes. Various bound protonated molecular ions, such as H_3^+, HCO^+, HCS^+, etc., have been identified in the interstellar medium through radio-astronomical spectra [1,2]. Inelastic and charge transfer processes are responsible for the formation of these protonated ionic species. Many sulfur containing diatomic and polyatomic molecules have been detected in dense interstellar clouds. Among them carbon monosulfide (CS), the first sulfur containing molecule, discovered in 1971 in the interstellar clouds and thioformyl cation, HCS^+, detected in 1981 have attracted attention in understanding the sulfur chemistry of the interstellar clouds [3,4]. Interstellar sulfur molecules are homologs to oxygen molecules, like CS and CO, HCS^+ and HCO^+. Similarly, CS^+ is an isovalent species of CO^+, where later has been detected in the interstellar medium. Both share presence in the atmospheres and comet tails [5]. CS^+ is an important precursor and an intermediate in the formation of HCS^+ and also participate in the formation of CS in the interstellar medium but it has not been conclusively identified [6,7]. Kinetics of CS^+ with abundant neutral molecules had been studied in laboratory where formation of HCS^+ is suggested to be an exothermic reaction using the precursor CS^+ ion [8].

Several chemical schemes have been proposed for the formation and dissociation of HCS^+ with its dissociative recombination mechanism. Gerones et al. have analyzed the HCS^+ formation and its high stability over the range of photon energies [9,10]. In the past, *ab initio* studies have been performed to obtain the spectroscopic properties of HCS^+ with its optimized structural parameters [11]. Configuration interaction (CI) method with triple-zeta basis sets has been employed to study HCS^+/HSC^+ isomerization in 1985 [12]. In 1991, Talaty et al. reported that the HCS^+ isomer is linear and global minimum while its HSC^+ isomer is bent and higher in energy [13]. Molecular properties, isomerization, and energetics of neutral CS, HCS/HSC and HCS^+/HSC^+ systems have been studied by Puzzarini [14]. Cotton et al. have performed structural and spectroscopic studies of CS-HCS^+ van der Waals complex [15]. The structural parameters, harmonic vibrational frequencies and charge distribution data of noble gas (Ng) inserted in the HCS^+ ion resulting in $HNgCS^+$ has been studied at the MP2, DFT and CCSD(T) level of methods [16]. Recently, the time-dependent wave packet dynamics and charge transfer processes have been reported between the one-dimensional ground state and the low-lying excited states potential energy surfaces (PESs) in collinear and perpendicular approaches of H towards CS^+ at the MRCI/aug-cc-pVQZ level of theory [17].

For detailed understanding of collision dynamics in terms of ro-vibrational cross section and rate coefficients in the ion-neutral system, it is necessary to construct reliable global PES, CS^+-H channel being the ground state PES of HCS^+. Present study emphasis on the construction of three dimensional PES of formation of HCS^+ and HSC^+ from attachment of H towards CS^+ from carbon as well as

sulfur end. For the first time, the ground state and the low-lying excited state PESs of HCS$^+$ have been generated using *ab initio* method and the surface has been analytically fitted. The details are discussed in Section 2. The multipolar expansion coefficients of potentials computed using rigid-rotor surface which is extracted from the full PES is described in Section 3. Finally the summary of the present work is provided in Section 4.

2. Computational details

2.1. Ab initio potential energy surfaces

Ab initio calculations have been performed for HCS$^+$ in Jacobi coordinates to compute interaction potential, where variables R and r represent the distance of hydrogen from center-of-mass of CS$^+$ and interatomic distance of CS$^+$, respectively, and $\gamma = cos^{-1}(R.r)$, is the angle between R and r as shown in Fig. 1. The method employed for the PES calculation is the internally contracted multireference configuration interaction (MRCI) as implemented in MOLPRO package [18]. The basis sets of Dunning's augmented correlation consistent polarized quadruple zeta (aug-cc-pVQZ) for H, C and S atoms are chosen [19]. The adiabatic ground state and the first excited state PESs are computed for orientations $0° \leqslant \gamma \leqslant 180°$ with $15°$ increment. While the second excited state PES is also computed for collinear ($\gamma = 0°$, $180°$) and perpendicular orientations ($\gamma = 90°$) as avoided crossings have been observed in one-dimensional PESs studied previously to investigate the non-adiabatic couplings present in the system using time-dependent wave packet dynamics [17]. For the C_s point group, the computations employed 210 contracted functions with 133 in a$'$ and 77 in a$''$ symmetry. The core orbitals having lowest 5 orbitals in a$'$ and one orbital in a$''$ is kept frozen and are taken from self-consistent field calculations. The active orbitals with 6–12 a$'$ and 1–2 a$''$ symmetry incorporate remaining 10 electrons in the complete active space self-consistent field (CASSCF) calculations. The MRCI calculations following CASSCF method generate reference space of 1589 configurations: N, N-1 and N-2 internal configuration consist of 2907, 3139 and 2907 configurations, respectively. Total number of contracted configurations, 2436680 include 2744 internal, 864556 singly external and 1569380 doubly external configurations.

The plots of computed PESs as a function of R and r at fixed γ for $0°$, $30°$, $75°$, $90°$, $120°$ and $180°$ orientations are shown in Figs. 2(a)–(f) as reference. The PESs are obtained with the set of grid points as follows: $R = 1.4(0.2)8.0$ and $8.0(0.4)11.2\ a_o$, $r = 2.1(0.1)3.5\ a_o$ and $\gamma = 0°(15°)180°$. The numbers written in parenthesis implies the increment in the stated intervals. The 1–3 $^1\Sigma^+$ and 1–3 $^1A'$ electronic states are computed for collinear ($\gamma = 0°$, $180°$) and perpendicular orientation ($\gamma = 90°$), respectively, while 1–2 $^1A'$ electronic states are computed for bent (off-collinear) approaches.
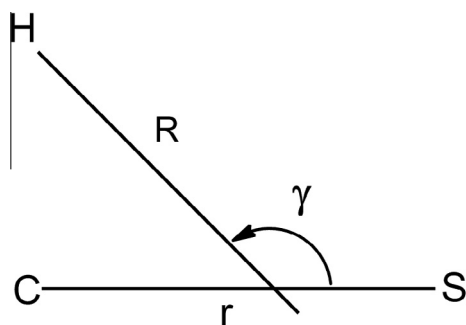

Fig. 1. Jacobi coordinates representation of H collision with CS$^+$.

A total of 8190 *ab initio* points have been computed with the variation in R, r, γ being 42, 15, 13 points, respectively. The ground state asymptotic channel corresponds to the H (^2S) + CS$^+$($X\ ^2\Sigma^+$) for both collinear and bent orientations. The first excited state (collinear – 2 $^1\Sigma^+$, bent – 2 $^1A'$) channel corresponds to the H$^+$ + CS ($X\ ^1\Sigma^+$) asymptote in collinear orientations while corresponds to higher energetic channel of the H (^2S) + CS$^+$ ($A\ ^2\Pi$) asymptote in bent orientations. The second excited state (collinear – 3 $^1\Sigma^+$, bent – 3 $^1A'$) channel corresponds to higher energetic channel of the H (^2S) + CS$^+$ (2 $^2\Sigma^+$) asymptote in collinear orientation while it corresponds to the H$^+$ + CS ($X\ ^1\Sigma^+$) asymptote in bent orientations. The asymptotic channels are confirmed through the computation of corresponding equilibrium geometries of ground and various excited states of the H + CS$^+$ and H$^+$ + CS systems. H + CS$^+$ channel is the lowest over H$^+$ + CS channel due to high ionization potential of H (13.6 eV) over CS (11.3 eV). In $180°$ orientation, the 2 $^1\Sigma^+$ state show avoided crossing with the 3 $^1\Sigma^+$ state while in bent $90°$ orientation, the 1 $^1A'$ state show avoided crossing with the 2 $^1A'$ state indicating presence of Landau–Zener coupling in the interaction region [20,21].

The electronic states of one-dimensional PESs of CS$^+$ for $X\ ^2\Sigma^+$ and $A\ ^2\Pi$ have been obtained and shown in Fig. 3. The dissociation energy for $X\ ^2\Sigma^+$ and $A\ ^2\Pi$ states are found to be 50950.9 cm^{-1} and 38047.0 cm^{-1}, respectively. Vibrational bound states have been obtained by solving 1D Schrödinger equation numerically using Le Roy code [22]. There are 58 vibrational levels for the $X\ ^2\Sigma^+$ state and 72 vibrational levels for the $A\ ^2\Pi$ state. The first 20 levels are provided in the Table 1 along with the experimental values and comparison of computed potential turning points with Rydberg–Klein–Rees (RKR) data [23] are given in Table 2.

2.2. Analytical fitting of the ground state surface

In order to analytically fit the ground state surface, the method of power series expansion in R and r has been tried to represent zeroth order harmonic nature of CS$^+$ vibration of the form:

$$V(R', r'; \gamma) = \sum_i \sum_j C_{ij}(R')^i (r')^j \tag{1}$$

where R', and r' are the Simons–Parr–Finlan [24] coordinates, related to the Jacobi distances R and r by $R' = 1 - \frac{R_{eq}}{R}$, and $r' = 1 - \frac{r_{eq}}{r}$, respectively, with R_{eq} and r_{eq} being equilibrium values. The potential is expanded around the local minimum. This type of fitting has been reported for the H$^+$ + N$_2$ system [25]. However, the expansions for R and r parts are valid if PES exhibit only one global minimum. In the H + CS$^+$ system there are two minima, one for bent approach of H towards the S-end ($\gamma = 75.2°$) and another for collinear approach of H towards the C-end ($\gamma = 180°$) and the above function is not reproducing the potential at longer R and r values resulting in large error. Therefore, the inverse power series expansion function has been tried to fit the ground state potential energy surface as a function of R and r at fixed values of γ of the form:

$$V(R, r; \gamma) = \sum_{i=0}^{7} \sum_{j=0}^{7-i} C_{ij} \left(\frac{1}{R}\right)^i \left(\frac{1}{r}\right)^j \tag{2}$$

The parameters C_{ij} for each orientation (γ) are optimized by minimizing the root mean square deviation of the values of the potential energy given by the analytical function from the numerical values. A set of 36 coefficients for each orientation ($\gamma = 0°$ ($15°$) $180°$) is found to give a good representation of the surface with the standard deviation of the fit to be in the range of 0.5–4.8 meV. The fitting coefficients, C_{ij}, for $\gamma = 0°$ ($15°$) $180°$ are listed in Table S1 as supporting information. The fortran code
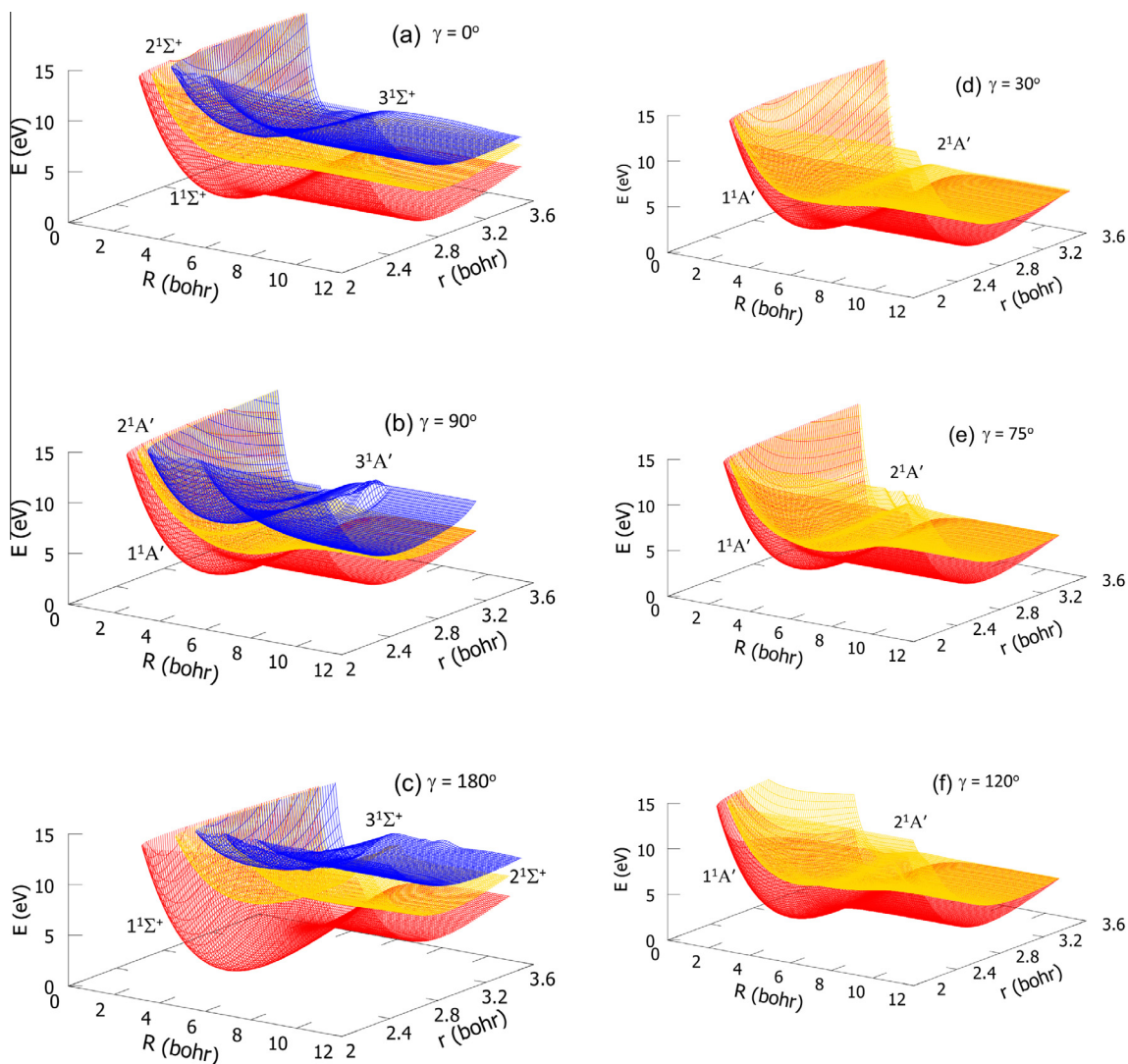
Fig. 2. The ground state (red) and the low-lying excited (yellow, blue) PESs as a function of R and r at various orientations (γ). (For interpretation of the references to color in this figure legend, the reader is referred to the web version of this article.)
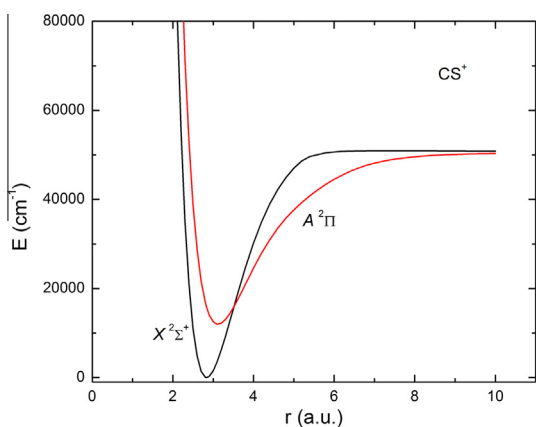

Fig. 3. Potential energy curves for the $X\ ^2\Sigma^+$ and $A\ ^2\Pi$ states of CS^+.

to generate the *ab initio* ground state PES of the system as a function of R and r at various fixed γ is available on request from the authors. The fitting coefficients reproduces reliable *ab initio* points in the range of r and R up to $3.5\ a_0$ and $10\ a_0$, respectively.

2.3. Stability of HCS⁺ and HSC⁺ ions

The various bond parameters of equilibrium geometries of HCS⁺ and HSC⁺ isomers obtained using the present MRCI method and the earlier reported values at the CCSD(T) method [14,26] and experimental values [26,27] of HCS⁺ are provided in Table 3. Good agreement can be seen between the available experimental values and theoretically computed values at the MRCI level of theory. From the computed *ab initio* surfaces the PES profile is generated by taking the difference of energy from minimum of the ground state potential energy well to their corresponding asymptotic potential for every angle (γ). A plot with calculated well depths for the H collision with S-end of CS⁺ ($\gamma = 0°$) to the H collision with C-end of CS⁺ ($\gamma = 180°$), is shown in Fig. 4. As one can observe along the minimum at each γ, there is no barrier to the rotation of the H from the S-end to the C-end of CS⁺ and the present results are validated with results reported by Bruna et al. in 1978 [28]. This might be the reason for the detection of HSC⁺ isomer in the interstellar medium unreported till date with small well-depth of 1.88 eV. Moreover, the linear HCS⁺ is highly stable relative to its isomeric form HSC⁺ by 4.21 eV (97 kcal/mol) whereas, this difference in energy reported earlier is 110 kcal/mol. This small energy difference between the present and the earlier reported value is due to the

Table 1
Vibrational levels for the $X\,^2\Sigma^+$ and $A\,^2\Pi$ states of CS$^+$ (in cm^{-1}) computed at the MRCI/aug-cc-pVQZ along with the experimental data [23].

v	$X\,^2\Sigma^+$		$A\,^2\Pi$	
	E_v	Expt.	E_v	Expt.
0	681.3	686.8	12466.3	12492.5
1	2032.8	2048.7	13456.8	13492.7
2	3369.1	3394.9	14434.0	14479.3
3	4690.0	4725.4	15397.8	15452.1
4	5995.6	6040.2	16348.2	16411.2
5	7285.9	7339.3	17285.0	17356.7
6	8560.8	8622.6	18208.3	18288.5
7	9820.3	9890.2	19117.9	19206.6
8	11064.4	11142.0	20013.9	20111.1
9	12293.0	12378.0	20896.1	21001.8
10	13506.1	13598.1	21764.4	21878.9
11	14703.7	14802.4	22618.8	22742.2
12	15885.7	15990.8	23459.0	
13	17052.2	17163.3	24285.1	
14	18202.9	18319.9	25096.8	
15	19337.9	19460.5	25893.9	
16	20457.2	20585.2	26676.5	
17	21560.5	21693.8	27444.2	
18	22648.0	22786.5	28197.1	
19	23719.6	23863.1	28934.9	

Table 2
Potential turning points for $X\,^2\Sigma^+$ and $A\,^2\Pi$ states of CS$^+$ computed at the MRCI/aug-cc-pVQZ along with RKR data [23]. The distances are in Å

v	$X\,^2\Sigma^+$				$A\,^2\Pi$			
	R_{min}	R_{max}	RKR R_{min}	RKR R_{max}	R_{min}	R_{max}	RKR R_{min}	RKR R_{max}
0	1.458	1.552	1.442	1.548	1.591	1.711	1.581	1.705
1	1.419	1.600	1.408	1.593	1.555	1.766	1.543	1.758
2	1.399	1.634	1.387	1.626	1.527	1.807	1.518	1.798
3	1.379	1.663	1.370	1.655	1.508	1.841	1.499	1.832
4	1.366	1.689	1.356	1.681	1.491	1.872	1.483	1.863
5	1.354	1.712	1.344	1.705	1.479	1.902	1.469	1.892
6	1.344	1.735	1.333	1.728	1.468	1.930	1.457	1.920
7	1.332	1.758	1.324	1.749	1.458	1.956	1.447	1.946
8	1.321	1.779	1.315	1.771	1.448	1.983	1.437	1.972
9	1.315	1.799	1.307	1.791	1.439	2.007	1.428	1.997
10	1.309	1.819	1.300	1.811	1.428	2.034	1.420	2.022
11	1.302	1.839	1.293	1.831	1.422	2.057	1.411	2.046
12	1.296	1.859	1.286	1.851				
13	1.291	1.879	1.280	1.870				
14	1.284	1.898	1.274	1.889				
15	1.277	1.917	1.269	1.908				
16	1.271	1.936	1.263	1.927				
17	1.267	1.956	1.258	1.946				
18	1.263	1.979	1.254	1.964				
19	1.258	1.993	1.249	1.983				

Table 3
Equilibrium geometry parameters of the HCS$^+$ and HSC$^+$ with earlier theoretical data and available experimental data.

Parameters	HCS$^+$			HSC$^+$		
	r_{HC} (a_0)	r_{CS} (a_0)	$\angle$HCS$^+$	r_{HS} (a_0)	r_{SC} (a_0)	$\angle$HSC$^+$
MRCI/aug-cc-pVQZ (present)	2.044	2.803	180.0°	2.632	3.061	75.2°
CCSD(T)/cc-pVQZ [14,26]	2.045	2.803	180.0°	2.638	3.061	74.7°
Experiment [27,26]	2.042	2.793	180.0°	–	–	–

choice of method and basis sets. Present data can be taken as more reliable as larger basis sets are employed in the calculation. HCS$^+$ has the minimum energy compared to HSC$^+$ with dissociation energy of 6.09 eV.

3. Rigid-rotor surface

The rigid-rotor PES has been chosen with the CS bond distance fixed at an experimental equilibrium distance [29] $r_{eq} = 2.900\ a_o$.

The rigid-rotor PES is described as a function of R and γ at r_{eq} shown in Fig. 5(a). Two-dimensional contour plot of the surface that asymptotically correlates to the CS$^+$($X\,^2\Sigma^+$) + H (^2S) is shown in Fig. 5(b). The numbers in the plot indicate the energy level of the contours in eV. From the plots, it can be seen that the global minimum, HCS$^+$ lies at $R = 4.0\ a_o$ and $\gamma = 180°$ (3.14 radians).

The rigid-rotor surface is fitted in the expansion of Legendre polynomials is as follows,

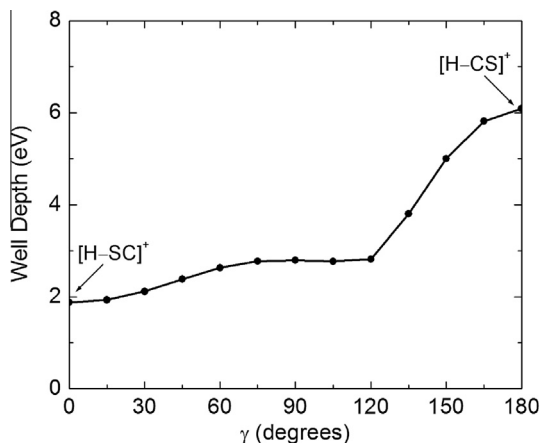**Fig. 4.** Variation in the ground state potential energy well in terms of well depth as a function of γ from 0° to 180°.
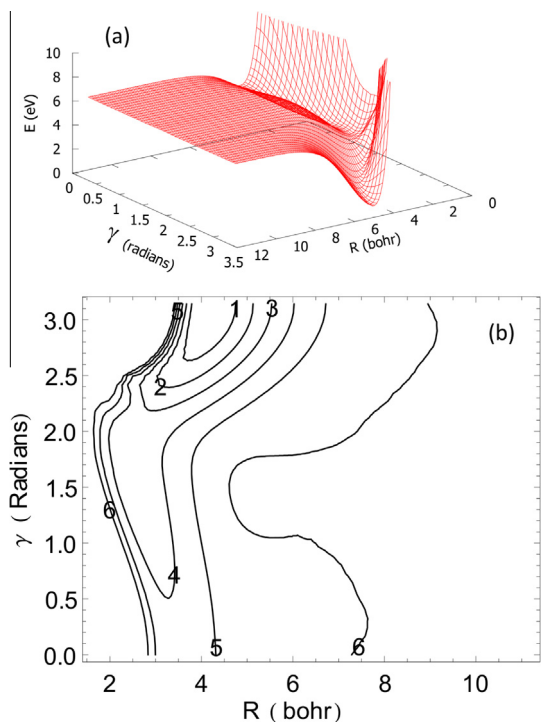

Fig. 5. (a) Rigid-rotor PES as a function of R and γ at fixed r_{eq} = 2.900 a_o and (b) the contour plot of rigid-rotor surface of the H–CS$^+$ system.

$$V(R, r = r_{eq}, \gamma) = \sum_{\lambda} V_{\lambda}(R) P_{\lambda}(\cos \gamma) \qquad (3)$$

where, P'_{λ} s are the Legendre polynomial functions. The multipolar expansion coefficients are computed for λ = 0 to 12 and the plots of 13 computed values of V_{λ} as a function of R are shown in Fig. 6. It can be seen from Fig. 6(a) for λ = 0–5 that V_0 and V_2 exhibit deep potential attractive wells. V_1 and V_3 display repulsive behavior with barriers. While V_4 has shallow well, V_5 show barrier-less repulsive behavior. The anisotropy of the interaction potential observed for V_{λ}, where λ = 6–12 is shown in Fig. 6(b). The magnitude of the coefficients decreases as the λ value increases. The coefficients obtained are interpolated using cubic spline method in the range of R = 1.4–11.2 a_0. The computed multipolar expansion coefficients indicate highly anisotropic nature of the rigid-rotor surface. The resulting V_{λ}'s can used for the kinetic study to compute various
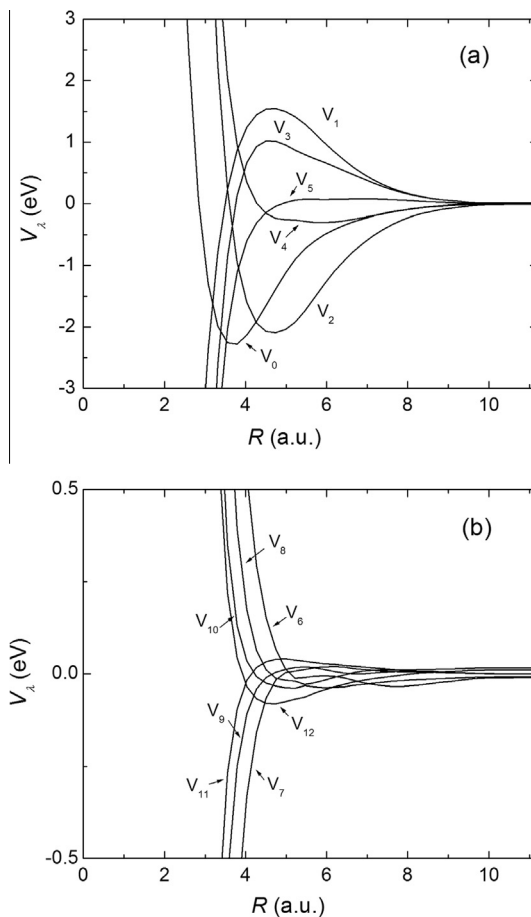

Fig. 6. Radial multipolar expansion coefficients for H–CS$^+$ system as a function of R at $r = r_{eq}$ with (a) the lower coefficients V_{λ} = 0–5 and (b) the higher coefficients V_{λ} = 6–12. A few lower even coefficients show attractive wells while odd coefficients show repulsive behavior with barrier.

dynamical parameters such as integral cross sections, and rate coefficients at low and ultracold collision energies. Tabulated values of V_{λ} fitting coefficients as a function of R are provided in Table S2 (λ = 0–5) and Table S3 (λ = 6–12) as supporting information. The effects of anisotropy in potentials can be well studied through rotational transition cross sections.

4. Summary and conclusions

Ab initio full PESs of HCS$^+$ molecular ion have been generated using the MRCI/aug-cc-pVQZ method. The ground state PES have been fitted analytically using inverse power series method. The ground state PES computed for various bent orientations reveals the stable configuration of linear HCS$^+$ with dissociation energy of 6.09 eV into H + CS$^+$. Potential energy profile of the system displays the barrier-less rotation of H from the S-end to the C-end of CS$^+$. Multipolar expansion coefficients computed from the surface indicate highly anisotropic nature of the system. The singlet surface along with triplet surface will be useful for the understanding of collision dynamics in terms of ro-vibrational cross sections and rate coefficients.

research fellowship. The calculations are carried out in IIT Ropar using High-Performance Computing cluster facility.

Appendix A. Supplementary data

Supplementary data associated with this article can be found, in the online version, at http://dx.doi.org/10.1016/j.chemphys.2016.09.015.

References

[1] E. Herbst, Chem. Soc. Rev. 30 (2001) 168.
[2] S.L.W. Weaver, D.E. Woon, B. Ruscic, B.J. McCall, Astrophys. J. 697 (2009) 601.
[3] A.A. Penzias, P.M. Solomon, R.W. Wilson, K.B. Jefferts, Astrophys. J. 168 (1971) L53.
[4] P. Thaddeus, M. Guelin, R.A. Linke, Astrophys. J. 246 (1981) L41.
[5] R. Lüst, Top. Curr. Chem. 99 (1981) 73.
[6] S.S. Prasad, W.T. Huntress, Astrophys. J. 260 (1982) 590.
[7] Y. Liu, C. Duan, J.J. Liu, L. Wu, C. Xu, Y. Chen, P.A. Hamilton, P.B. Davies, J. Chem. Phys. 116 (2002) 9768.
[8] J. Barassin, R. Thomas, A. Barassin, J. Chem. Phys. 79 (1983) 1546.
[9] M. Gerones, M.F. Erben, R.M. Romano, R.L.C. Filho, C.O.D. Vedova, J. Phys. Chem. A 114 (2010) 12353.
[10] M. Gerones, M.F. Erben, R.M. Romano, R.L.C. Filho, C.O.D. Vedova, J. Phys. Chem. A 116 (2012) 2571.
[11] P. Botschwina, P. Sebald, J. Mol. Spectrosc. 110 (1985) 1.
[12] S.A. Pope, I.H. Hillier, M.F. Guest, J. Am. Chem. Soc. 107 (1985) 3789.
[13] E.R. Talaty, Y. Huang, M.E. Zandler, J. Am. Chem. Soc. 113 (1991) 779.
[14] C. Puzzarini, J. Chem. Phys. 123 (2005) 024313.
[15] C.E. Cotton, J.S. Francisco, R. Linguerri, A.O. Mitrushchenkov, J. Chem. Phys. 136 (2012) 184307.
[16] A. Ghosh, D. Manna, T.K. Ghanty, J. Phys. Chem. A 119 (2015) 2233.
[17] R. Kaur, T.J.D. Kumar, Mol. Phys. 113 (2015) 3271.
[18] H.-J. Werner, P. J. Knowles, G. Knizia, F. R. Manby, M. Schütz, P. Celani, T. Korona, R. Lindh, A. Mitrushenkov, G. Rauhut, K. R. Shamasundar, T. B. Adler, R. D. Amos, A. Bernhardsson, A. Berning, D. L. Cooper, M. J. O. Deegan, A. J. Dobbyn, F. Eckert, E. Goll, C. Hampel, A. Hesselmann, G. Hetzer, T. Hrenar, G. Jansen, C. Köppl, Y. Liu, A. W. Lloyd, R. A. Mata, A. J. May, S. J. McNicholas, W. Meyer, M. E. Mura, A. Nicklass, D. P. O'Neill, P. Palmieri, D. Peng, K. Pflüger, R. Pitzer, M. Reiher, T. Shiozaki, H. Stoll, A. J. Stone, R. Tarroni, T. Thorsteinsson, M. Wang, MOLPRO, version 2012.1, a package of ab initio programs 2012, see http://www.molpro.net.
[19] T.H. Dunning, J. Chem. Phys. 1007 (1989) 90.
[20] C. Zener, Proc. R. Soc. Lond. Ser A 137 (1932) 696.
[21] H. Nakamura, in: R.E. Wyatt, J.Z.H. Zhang (Eds.), Dynamics of Molecules and Chemical Reactions, Marcel Dekker, New York, 1996, Chap. 12, p. 474.
[22] R.J. Le Roy, University of Waterloo Chemical Physics Research Report, Report CP-55R, University of Waterloo, Waterloo, Ontario, Canada, 1996.
[23] Y.Y. Liu, C.X. Duan, J.J. Liu, L. Wu, C.X. Xu, Y.Q. Chen, P.A. Hamilton, P.B. Davies, J. Chem. Phys. 116 (2002) 9768.
[24] G. Simons, R.G. Parr, J.M. Finlan, J. Chem. Phys. 59 (1973) 3229.
[25] S. Mahapatra, R. Vetter, Ch. Zuhrt, H.T. Nguyen, T. Ritschel, L. Zülicke, J. Chem. Phys. 107 (1997) 2930.
[26] L. Margules, F. Lewen, G. Winnewisser, P. Botschwina, H.S.P. Muller, Phys. Chem. Chem. Phys. 5 (2003) 2770.
[27] B. Ruscic, J. Berkowitz, J. Chem. Phys. 98 (1993) 2568.
[28] P.J. Bruna, S.D. Peyerimhoff, R. Buenker, J. Chem. Phys. 27 (1978) 33.
[29] K.P. Huber, G. Herzberg, Constants of Diatomic Molecules, Van Nostrand, New York, 1979.